Simulation Studies of the Interfaces of Incompatible Glycidyl Azide Polymer/Hydroxyl-Terminated Polybutadiene Blends by Dissipative Particle Dynamics. I. The Effect of Block Copolymers and Plasticizers

Yang Zhou,[1,2] Xin-Ping Long,[3] Qing-Xuan Zeng[1]

[1]*School of Mechanical and Electrical Engineering, Beijing Institute of Technology, Beijing, 100081, China*
[2]*Institute of Chemical Materials, Chinese Academy of Engineering and Physics, Mianyang, 621900, China*
[3]*Chinese Academy of Engineering and Physics, Mianyang, 621900, China*

Received 10 July 2011; accepted 13 October 2011
DOI 10.1002/app.36370
Published online 15 January 2012 in Wiley Online Library (wileyonlinelibrary.com).

ABSTRACT: Dissipative particle dynamics (DPD) simulations were used to investigate the interfaces of incompatible glycidyl azide polymer (GAP)/hydroxyl-terminated polybutadiene (HTPB) blends in the presence of block copolymers and plasticizers. They were GAP-*b*-HTPB copolymers and commonly used nitrate ester or inert plasticizers in the formulations of propellants. The results show that there were two abilities that determined the effects of the block copolymers and plasticizers on reducing the interfacial tension (γ). These were the penetrability into each homopolymer phase and the ability for assembling at the interface. The plasticizers mainly depended on the first ability, and the block copolymers depended on the other ability. In addition, block copolymers with the different chain lengths had the different influences on γ of the GAP/HTPB blends. Moreover, this phenomenon could also be explained by the above two abilities. © 2012 Wiley Periodicals, Inc. J Appl Polym Sci 125: 1530–1537, 2012

Key words: adhesives; computer modeling; miscibility

INTRODUCTION

Composite solid propellants are a major resource for space vehicles and missiles. Their formulations generally include a binder, a plasticizer, a high-energetic filler, bonding and curing agents, a burning rate modifier, and so on. These additives are used mainly to satisfy the requirements of mechanical, ballistic, and processing characteristics of the propellants.[1] However, many conventional propellants have some limitations that cannot be improved. For example, the AP-based propellants can result in the exhaust of 220 tons of HCl from a single launch of a U.S. space shuttle and tremendous environmental pollution hazards.[2] Therefore, the search for new propellants is still a hot topic.

Recent advances for propellants include energetic binders that perform better than the common binder hydroxyl-terminated polybutadiene (HTPB). Among them, glycidyl azide polymer (GAP) is one of the most thoroughly studied energetic binders, and since shortly after its first synthesis in 1972 by Vandenberg,[3] its synthesis, performances and applications have been reported in detail by several works.[4–9] The major advantages of GAP over HTPB include a high-energy output, high density, and good compatibility with high energetic oxidizers, such as ammonium dinitramide (ADN) and hydrazinium nitroformate (HNF);[10] these result in higher specific impulses when it is used in propellant formulations. However, GAP suffers from poor low-temperature properties; its critical temperature (6°C) and glass-transition temperature (−43°C) are higher than those of HTPB because of its low weight percentage of polymer weight-bearing chain.[11] Therefore, the application of GAP will be significantly restricted if this demerit cannot be overcome effectively. It is natural idea that GAP should be improved its blending with other binders having good mechanical properties, especially HTPB. However, GAP/HTPB blends without any additives still have poor mechanical characteristic because of their immiscibility. There is an obvious phase separation when a mixture of pure GAP and HTPB is kept undisturbed for a while after dispersion. In fact, this defect of GAP/HTPB blends can be partly improved by the use of curing agents[10–13] which can also form network structures and increase the contents of solid energetic materials. However, the remnant GAP and HTPB can phase-

Correspondence to: Z. Yang (zhouy@caep.ac.cn).
Contract grant sponsor: Foundation of Chinese Academy of Engineering and Physics; contract grant numbers: 2010A03002, 2011A030214.
Contract grant sponsor: National Nature Sciences Foundation of China; contract grant numbers: 10832003, 51173173, 21173199.

separate if the curing reactions are incomplete. At the moment, the influences of GAP/HTPB interfacial properties on the whole systems cannot be neglected, and block copolymers from the curing reactions behave as a classical surfactants that can tailor the interfacial properties. Therefore, the mechanical properties of GAP/HTPB blends seriously depend on the contents of the curing agents (NCO/OH ratio).[10,14–17] In addition, the bond performances between HTPB liner and GAP propellants are a key factor determining the safety of rocket engines and are also related to the interfacial properties of GAP/HTPB. Provatas[4] found that when they were cured with isocyanate, polyurethane rubbers showed poor stability. These problems impelled us to find other methods to increase the miscibility of GAP and HTPB, such as the addition of block copolymers. Apart from these, we needed to determine whether the necessary plasticizers of the propellant formulations [e.g., nitrate ester (NE) or inert plasticizers] could also behave as the surfactants and effectively improve the interfacial properties of GAP/HTPB blends. Thus, we needed to study the effect of block copolymers and plasticizers on the interface of the GAP/HTPB blends in detail. Studies of this nature depending on experiments are expensive and dangerous. Therefore, computer simulation is a good choice because computer simulations are now capable of providing valuable microscopic and mesoscopic insights into the interfacial behaviors of the immiscible polymer blends, especially dissipative particle dynamics (DPD) simulation.[17–27] Comparisons with experimental and several theoretical studies have proven that DPD is intrinsically promising in the simulations of two phases with correctly defined interfaces.[28] In this study, by means of DPD simulation, we provided a first detailed mesoscale understanding of the interface of incompatible GAP/HTPB blends in the presence of block copolymers and plasticizers.

SIMULATION DETAILS

DPD method

The DPD method is a coarse-grained particle-based dynamics simulation technique that allows the simulation of the hydrodynamics behavior in mesoscale systems up to the microsecond range.[29–31] The interaction between DPD particles can be expressed by a conservative force (F^C), a dissipative force (F^D), a random force (F^R), and a harmonic spring force (F^S). The total force exerted on particle i (f_i) is given by

$$f_i = \sum_{j \neq i} (F_{ij}^C + F_{ij}^D + F_{ij}^R + F_{ij}^S) \tag{1}$$

The different parts of the three forces describing the nonbonded interaction are given by

$$\begin{aligned} F_{ij}^C &= -a_{ij} w^C(\boldsymbol{r_{ij}}) \boldsymbol{e_{ij}} \\ F_{ij}^D &= -\gamma w^D(\boldsymbol{r_{ij}})(\boldsymbol{e_{ij}} \cdot \boldsymbol{v_{ij}}) \boldsymbol{e_{ij}} \\ F_{ij}^R &= \sigma w^R(\boldsymbol{r_{ij}}) \xi_{ij} \Delta t^{-0.5} \boldsymbol{e_{ij}} \end{aligned} \tag{2}$$

where Δt is the time step, $\boldsymbol{r_{ij}} = \boldsymbol{r_i} - \boldsymbol{r_j}$, $\boldsymbol{r_{ij}} = |\boldsymbol{r_{ij}}|$, $\boldsymbol{e_{ij}} = \boldsymbol{r_{ij}}/\boldsymbol{r_{ij}}$, and $\boldsymbol{v_{ij}} = \boldsymbol{v_i} - \boldsymbol{v_j}$. ζ_{ij} is a random number with zero mean and unit variance. α_{ij} is the maximum repulsion that reflects the chemical characteristics of the interacting particles. γ and σ are interpreted as the friction coefficient and the amplitude of the noise, respectively. w^C, w^D, and w^R are three weight functions. For w^C, a simple form is chosen as $w^C(r_{ij}) = 1 - r_{ij}$ for $r_{ij} < 1$ and $w^C(r_{ij}) = 0$ for $r_{ij} \geq 1$. Unlike w^C, w^D and w^R have a certain relation to satisfy the fluctuation–dissipation theorem:[31]

$$w^D(r_{ij}) = [w^R(r_{ij})]^2, \quad \sigma^2 = 2\gamma k_B T \tag{3}$$

where w^D and w^R also use the simple form as same as w^C according to Groot and Warren.[32] In addition, the forces describing the connected particles are obtained by the differential of the spring potential:

$$\begin{aligned} F_{(i,i+1)}^S &= -\nabla U_{(i,i+1)}^S, \\ U_{(i,i+1)}^S &= \sum_i 1/2 k_S [l_{(i,i+1)} - l_0]^2 \end{aligned} \tag{4}$$

where $l_{(i,i+1)}$ is the bond length between the two connected particles i and $i + 1$, l_0 is the balance bond length and k_s is the spring coefficient. In DPD, the particles connected by the spring force can be used to represent the polymer. The simulations were performed with the DPD program of Materials Studio software (Accelrys, San Diego, USA), and we chose the radius of interaction, particle mass, and temperature as $r_c = m = k_B T = 1$, $\sigma = 3$ (where r_c is the interaction radius and m is the chain length) according to the defaults of the program. However, the repulsion parameter between the same particles (a_{ij}) could be mapped onto Flory–Huggins theory through the relation $a_{ij} = a_{ii} + 3.27\chi$ ($\rho = 3$), where a_{ii} has the value of $25 k_B T$, which gives a pure DPD fluid with a compressibility similar to that of liquid water.[32] The Flory–Huggins interaction parameter χ is defined as $\chi = z\Delta\omega_{12}/RT$, where z is the coordination number of the model lattice, R is the gas constant and $\Delta\omega_{12}$ is the energy of formation of an unlike pair and is defined as $\Delta\omega_{12} = \omega_{12} - (\omega_{11} + \omega_{22})/2$, where ω_{ij} is the energy of a particular ij pair. Further details can be found in the works by Fan et al.[33] and Schweizer and Curro.[34]

Coarse-graining strategy and simulation parameters

The molecular structures and coarse-grained models of the binder GAP and HTPB are given in Figure 1. The azido group ($-N_3$) in the side chain of GAP

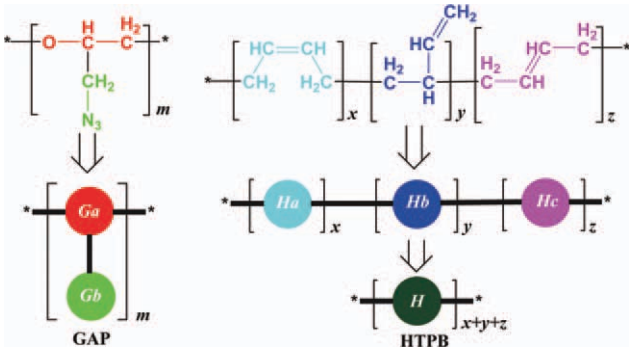

Figure 1 Molecular structures and coarse-grained models of GAP and HTPB. [Color figure can be viewed in the online issue, which is available at wileyonlinelibrary.com.]

can remarkably decrease the flexibility and weight percentage of the polymeric weight bearing chain; this is the main reason for the poor low-temperature mechanical properties.[35] Hence, GAP is coarse-grained as a short-brush model with beads G_a (—$OCHCH_2$—) and G_b (—CH_2N_3) (Fig. 1). The three different repeat units (*cis*-2,3-butadiene, 1,2-butadiene, and *trans*-2,3-butadiene) of HTPB are represented by H_a, H_b, and H_c, respectively. The molecular weights of GAP ($m = 20$, weight-average molecular weight ≈ 2000) and HTPB ($x + y + z = 55$, weight-average molecular weight ≈ 3000) were chosen on the basis of several experimental works.[11,16,36] To study the effects of the addition of block copolymers on the interfacial characteristics of the immiscible GAP/HTPB blends, two block copolymer GAP-*b*-HTPBs with different lengths ($m = 20$, $x + y + z = 55$, and $m = 10$, $x + y + z = 28$) were used. The coarse-grained models of four plasticizers are shown in Figure 2. The coarse grain of plasticizers follows two principles: the first is to keep their characteristic groups, such as —ONO_2, and the second is to guarantee that the volume of coarse-grained beads is close to the beads representing the binders GAP and HTPB. The two NE plasticizers [nitroglycerin (NG) and trimethyol ethane trinitrate (TMETN)] were coarse-grained and are shown in Figure 2(a,b), and the two inert plasticizers [dibutyl phthalate (DBP) and dioctyl adipate (DOA)] were also coarse-grained and are shown in Figure 2(c,d).

After the coarse-grained models were constructed, the next step was to calculate a_{ij} on the basis the previous relation, $a_{ij} = a_{ii} + 3.27\chi_{ij}$. First, the structures of all of the beads were optimized with molecular mechanics (Forcite module in Materials Studio) with COMPASS parameters. Second, the Flory–Huggins χ_{ij} parameters between these beads (G_a, G_b, H_a, H_b, H_c, N_e, N_a, N_b, N_c, B, D_o, D_a, and D_b) were calculated at room temperature with COMPASS force field parameters by the previous method, $\chi_{ij} = z\Delta\omega_{12}/RT$ (Blends module in Materials Studio). In this method, several interactions were considered, including electronic, Van der Waals, and hydrogen-bond interactions. The computed a_{ij} values are listed in Table I.

A cubic simulation box of 50^3 with periodic boundary conditions of three directions was applied; this was large enough to prevent finite size effects. A value of Δt of 0.05 was used, and a total of 2×10^5 DPD steps were carried out for all DPD simulations. In this study, the chosen beads had an average volume of 33.5 Å^3. Following the method of Groot and Rabone,[37] we determined r_c to be about 4.64 Å, and the simulated Δt was about 3.06 ps.[38] In this study, we mainly focused on the interfacial thermodynamic properties instead of the segregation kinetics of the blends. Therefore, in the initial configurations, two homopolymer binders were placed in the distinct half of the box along the x direction, that is, GAP in the left half of the box and HTPB in the right half. Consequently, the formed interface was perpendicular to the x direction. These artificial initial configurations could speed up the formation of the interface and, hence, save the computational cost. The block copolymers and plasticizers in the ternary systems were randomly placed in the box.

RESULTS AND DISCUSSION

Effect of the chain length and concentration of block copolymer

The fine control of the interface is very important in tailoring the basic properties of such unmixed

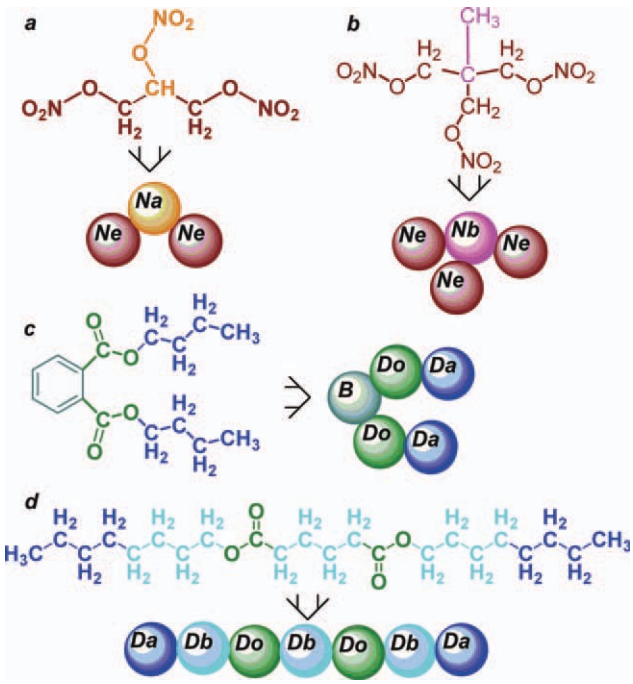

Figure 2 Coarse-grained models of (a) NG, (b) TMETN, (c) DBP, and (d) DOA. [Color figure can be viewed in the online issue, which is available at wileyonlinelibrary.com.]

TABLE I
Computed a_{ij} Values Describing the Pairwise Interactions for the Different Beads

	a_{ij}											
	G_a	G_b	H_a	H_b	H_c	N_a	N_b	N_e	B	D_a	D_b	D_o
G_a	25.0	—	—	—	—	—	—	—	—	—	—	—
G_b	26.4	25.0	—	—	—	—	—	—	—	—	—	—
H_a	34.0	30.9	25.0	—	—	—	—	—	—	—	—	—
H_b	35.0	31.9	25.0	25.0	—	—	—	—	—	—	—	—
H_c	34.7	31.7	25.0	25.0	25.0	—	—	—	—	—	—	—
N_a	29.4	25.5	34.3	35.4	35.4	25.0	—	—	—	—	—	—
N_b	35.8	33.6	26.7	26.9	26.6	—	25.0	—	—	—	—	—
N_e	29.8	25.7	35.5	36.7	36.8	24.7	40.4	25.0	—	—	—	—
B	27.7	26.3	24.8	24.8	25.1	—	—	—	25.0	—	—	—
D_a	35.9	32.5	25.2	25.0	25.0	—	—	—	25.3	25.0	—	—
D_b	35.7	32.5	25.2	25.1	25.1	—	—	—	25.5	25.0	25.0	—
D_o	27.8	43.5	77.2	80.8	80.8	—	—	—	37.8	25.3	25.5	25.0

polymer systems. In this section, the effects of the block copolymer GAP-*b*-HTPB on the interfacial properties are discussed, and the results are shown in Figures 3 and 4. Figure 3 shows the relation between the simulated interfacial tension (γ) and the concentration of the GAP-*b*-HTPB block copolymers. Apparently, γ decreased rapidly with increasing concentration of GAP-*b*-HTPB, regardless of the chain length; however, there was no linear relationship. Moreover, from Figures 4 and 5, we can clearly see the interface structures and the aggregation phenomena of the GAP-*b*-HTPB block copolymers. The two figures show that the interface of the incompatible GAP/HTPB blends was located at approximately $x = 25$, wherein the densities of the homopolymer binders GAP and HTPB abruptly decreased (Fig. 4) and the densities of the GAP-*b*-HTPB block copolymers suddenly appeared as two peaks (Fig. 5). One of them was the accumulation of GAP blocks at the interfacial side closing with the homopolymer GAP phase. The other was that HTPB segments accumulated at the side of the homopolymer HTPB phase. It was the accumulation of GAP-*b*-HTPB block copolymers at two sides of the interface that pushed each homopolymer further away from the interface; this made the interfacial width broaden with increasing concentration of block copolymers, as shown in Figure 4. These two results (the decrease of γ and the increase of the interfacial width) are familiar phenomena when one uses the addition the amphiphilic surfactants or block copolymers to improve the interfacial properties. However, we also found an unusual phenomenon from Figure 3, which could be divided into two classes by the divided point $f_{\text{GAP-}b\text{-HTPB}} = 0.19$ (the concentration of GAP-*b*-HTPB). From area I, we can see that for block copolymers with a fixed

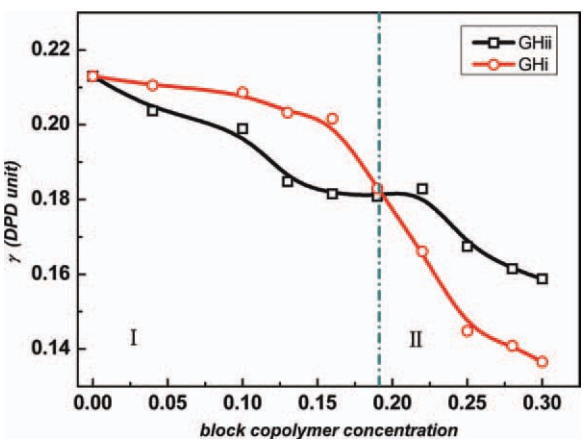

Figure 3 γ values for GAP/HTPB/GAP-*b*-HTPB blends at different block copolymer concentrations, wherein GHi represents the block copolymer GAP-*b*-HTPB with $m = 20$ and $x + y + z = 55$ and GHii represents the block copolymer GAP-*b*-HTPB with $m = 10$ and $x + y + z = 28$. [Color figure can be viewed in the online issue, which is available at wileyonlinelibrary.com.]

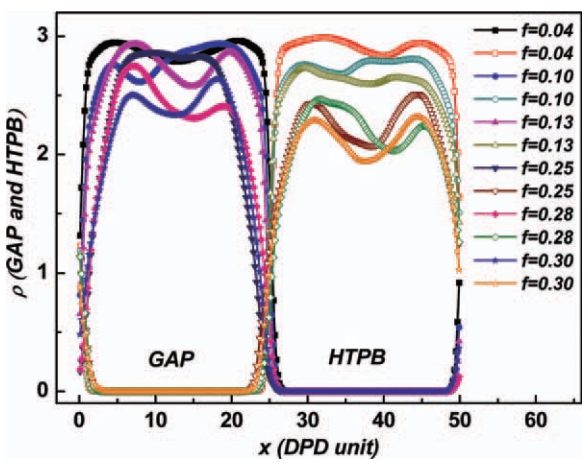

Figure 4 Density profiles of the homopolymer segments in the ternary GAP/HTPB/GAP-*b*-HTPB systems. Science block copolymers with different chain lengths have a similar rule. This figure shows only one result for longer chains ($m = 20$, $x + y + z = 55$). ρ_{GAP} is represented by solid symbols, and ρ_{HTPB} is represented by open symbols. [Color figure can be viewed in the online issue, which is available at wileyonlinelibrary.com.]

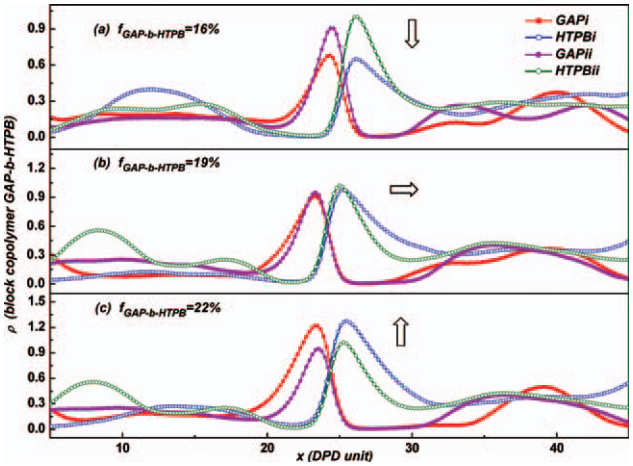

Figure 5 Density profiles of the block copolymer segments in the ternary GAP/HTPB/GAP-*b*-HTPB systems. In the block copolymer GAP-*b*-HTPB, the concentrations of GAPi ($m = 20$) and GAPii ($m = 10$) segments are represented by solid symbols (■ and ●), respectively. The concentrations of HTPBi ($x + y + z = 55$) and HTPBii ($x + y + z = = 28$) are represented by open symbols (□ and ○), respectively. [Color figure can be viewed in the online issue, which is available at wileyonlinelibrary.com.]

volume fraction, shorter chains (GHii) were be more efficient than the longer ones (GHi) in reducing γ. That is, GAP-*b*-HTPB with GHii made γ decrease more than GAP-*b*-HTPB with longer chains (GHi). The results were interpreted in the work by Qian et al.[28] as follows: when the chain length of the block copolymers increased at the fixed concentration, the surface density (SD; number of surfactants at the interface per area) decreased. Thus, the interactions between the block copolymer molecules were weaker, and the γ reduction effect decreased. However, area II shows the contrary result that the effect of GHi on reducing γ was more prominent than shorter ones (GHii), this seemed contradictory to the previous interpretation. To thoroughly investigate the unusual phenomena, we determined the simulated concentration profiles of block copolymer segments, as shown in Figure 5. Figure 5(a) ($f_{GAP\text{-}b\text{-}HTPB} = 0.16$ before the divided point) shows that the concentration of the copolymer blocks with GHii was higher than that of GHi near the interface. When $f_{GAP\text{-}b\text{-}HTPB} = 0.19$ was the dividing point [Fig. 5(b)], the concentration of GHii was nearly equal to that of GHi. Then, $f_{GAP\text{-}b\text{-}HTPB} = 0.22$ went beyond the divided point, there was a contrary distribution, in which the concentration of GHi was higher than that of GHii. Therefore, we could explain why block copolymers with GHi had a better efficiency in reducing γ than those with GHii (the unusual phenomena is shown in area II of Fig. 3) on the basis of the viewpoints of Qian et al.[28] The main reason was still related to SD. Longer GAP-*b*-HTPBs had larger SDs than the shorter ones when $f_{GAP\text{-}b\text{-}HTPB}$ exceeded a certain value (it was 0.19 here); this resulted in a higher efficiency in reducing γ. This also altered our routine viewpoint that GHii should accumulate more at the interface because there were greater molar numbers for GHii when the concentration was fixed.

To further clarify the reason for the changes in the density distribution, the concentrations of the terminal beads (G_{bb} and H_{bb}) for the block copolymers with different chain lengths are shown in Figure 6. As more block copolymers were added, Figure 6(a) shows that the terminal beads G_{bb} and H_{bb} of GHi had an increasing distribution along the interface. However, G_{bb} and H_{bb} of GHii showed a gentle increase perpendicular to the interface. This indicated that the block copolymer GAP-*b*-HTPB with longer chain length preferred to orient along the interface direction. This could also explain the reason why the concentration of GHi at the interface was greater than that of GHii after a given concentration, which was 0.19 in this work.

Effect of the plasticizers

Two NE plasticizers (NG and TMETN) and two inert plasticizers (DBP and DOA) were chosen to

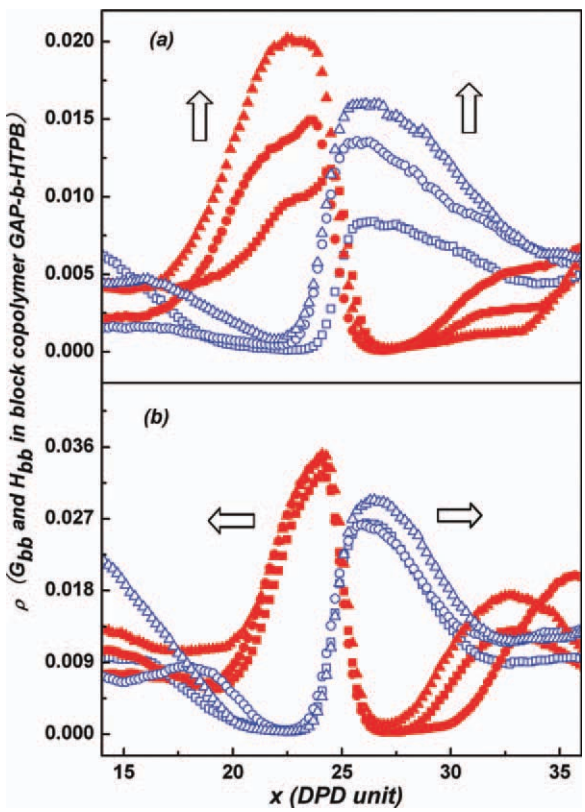

Figure 6 Density profiles [ρ_{Gaa} at $f_{GAP\text{-}b\text{-}HTPB}$ = (■) 0.16, (●) 0.19, and (▲) 0.22, and ρ_{Hbb} at $f_{GAP\text{-}b\text{-}HTPB}$ = (□) 0.16, (○) 0.19, and (△) 0.22] of the block copolymer [(a) GHi ($m = 20$, $x + y + z = = 55$) and (b) GHii ($m = 10$, $x + y + z = = 28$)] end beads in the ternary GAP/HTPB/block copolymer systems. [Color figure can be viewed in the online issue, which is available at wileyonlinelibrary.com.]

TABLE II
γ Values of the GAP/HTPB Blends in the Presence of Different Plasticizers

f	NG	TMETN	DOA	DBP
0.04	0.217	0.209	0.184	0.157
0.22	0.218	0.171	0.101	0.055
0.30	0.212	0.166	0.059	0.067

investigate the influence of small molecular plasticizers on the interface of the immiscible GAP/HTPB blends, respectively. The calculated results for the influence of different plasticizers on γ are listed in Table II. The results show that NG had hardly any influence on γ of the GAP/HTPB blend. However, TMETN could decrease γ stepwise with the addition of the content of TMETN; similar trends could also found for the inert plasticizers DOA and DBP. It was different that the influence of DBP on γ was not stepwise. γ no longer decreased when DBP exceeded a concentration limitation, which was approximately in the range 0.22–0.30 here. To get insight into these different influences of the small molecular plasticizers on γ, their density profiles were investigated and are given in Figure 7–10, respectively.

From Figure 7, we can see that the NG plasticizer showed no obvious aggregation at the interface of the GAP/HTPB blends. However, the other three plasticizers (TMETN, DOA, and DBP) showed obvious aggregation at the interface, as shown in Figure 8, 9, and 10, respectively. The different repulsive interactions (α_{ij}) between the coarse-grained beads of the plasticizers and binders were the main reason for the different aggregation behaviors at the interface. In general, when the repulsive interaction parameter (α_{AB}) was very close to or slightly greater than 25 ($\rho = 3$), we simply believe that the systems

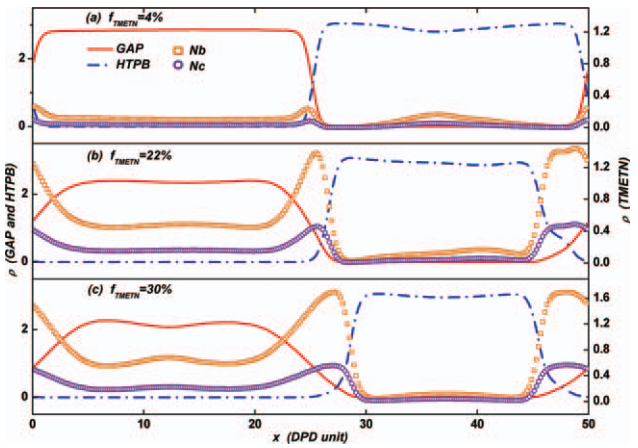

Figure 8 Density profiles for the ternary GAP/HTPB/TMETN systems. The *y* axis (right) in the same scale (a–c) is for the homopolymer GAP and HTPB, and the *y* axis (left) is for the plasticizer TMETN. [Color figure can be viewed in the online issue, which is available at wileyonlinelibrary.com.]

represented by them (A and B) were compatible or microcompatible. When α_{AB} was apparently greater than 25, the systems were incompatible. For the compatible or microcompatible systems, we said that A was B-like. For example, NG had two coarse-grained beads (N_a and N_e) that were all GAP-like, not HTPB-like, because the repulsive parameters between the beads of NG and GAP ($\alpha_{NeGa} \approx \alpha_{NaGa} \approx 29$ and $\alpha_{NeGb} \approx \alpha_{NaGb} \approx 25$) were far less than those between NG and HTPB ($\alpha_{NeHa} \approx \alpha_{NeHb} \approx \alpha_{NeHc} \approx 36$ and $\alpha_{NaHa} \approx \alpha_{NaHb} \approx \alpha_{NaHc} \approx 35$), as shown in Table I. This made the NG plasticizer prefer to distribute itself in the GAP phase and not to aggregate at the interface. Therefore, the density of beads N_a and N_e representing NG plasticizer had no obvious peak but had a definite distribution in the

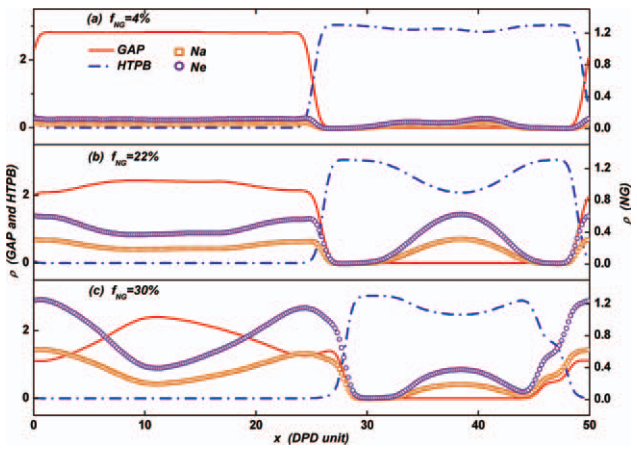

Figure 7 Density profiles for the ternary GAP/HTPB/NG systems. The *y* axis (right) in the same scale (a–c) is for the homopolymer GAP and HTPB, and the *y* axis (left) is for the plasticizer NG. [Color figure can be viewed in the online issue, which is available at wileyonlinelibrary.com.]

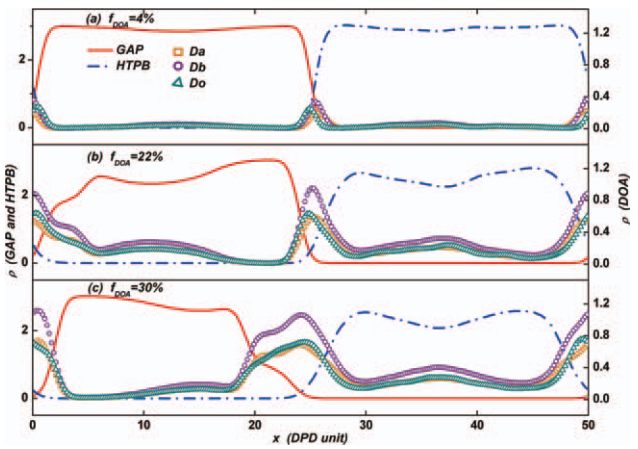

Figure 9 Density profiles for the ternary GAP/HTPB/DOA systems. The *y* axis (right) in the same scale (a–c) is for the homopolymer GAP and HTPB, and the *y* axis (left) is for the plasticizer DOA. [Color figure can be viewed in the online issue, which is available at wileyonlinelibrary.com.]

left GAP domain; this provided an explanation for why the NG plasticizers had no effect on reducing γ. For TMETN, it also had two coarse-grained beads (N_b and N_e). The previous analysis showed that N_e was GAP-like. However, on the basis of the data listed in Table I, we could testify that N_b was HTPB-like for the repulsive parameters, with $\alpha_{NbGa} \approx 36$ and $\alpha_{NbGb} \approx 34$ being greater than $\alpha_{NbHa} \approx \alpha_{NbHb} \approx \alpha_{NbHc} \approx 27$. Two types of beads (GAP- and HTPB-like) in TMETN would result in a competition of the distribution in the two phases (GAP and HTPB). The final results were that more TMETN plasticizers gathered at the interface, and Figure 8 displays that the density peak of beads N_b and N_e were higher with the gradual increase of TMETN content. It was the ability to assemble at the interface that made TMETN have a higher efficiency than NG on reducing γ. For the DOA and DBP plasticizers, there was a similar reason to TMETN. Through comparing the repulsive parameters in Table I, we determined that D_a and D_b were HTPB-like beads, D_o was GAP-like, and B was all-like. The DOA plasticizer had two HTPB-like beads (D_a and D_b) and one GAP-like bead (D_o). More HTPB-like beads finally resulted in the obvious distribution in the HTPB phase except for the aggregation of DOA at the interface (see Fig. 9). For the absence of the HTPB-like bead D_b, DBP had almost average distributions in the two separated phases and an obvious accumulation at the interface due to the balance between the numbers of GAP- and HTPB-like beads (see Fig. 10).

However, this analysis could not explain why the influence of DBP on γ was not stepwise with the increasing of its concentration. To explore the problem, we compared the distribution at the interface for the DBP and DOA plasticizers, as shown in Figure 11. Figure 11(b) shows that the peak width of DOA gradually broadened; this could show that the DOA plasticizers penetrated more deeply into the respective homopolymer phase with increasing concentration; similar results are also shown in Figure 9. From Figure 11(a), we can see that the DBP plasticizer had also this rule only when the variation of f_{DBP} was in the range 0.04–0.22. However, when f_{DBP} increased from 0.22 to 0.3, the peak width hardly had any expansions; this showed that its ability to penetrate into the homopolymer phase disappeared. This could be an explanation for why the influence of DBP on γ was not stepwise with the increase in its concentration. The main reason was the disappearance of the penetrability when f_{DBP} exceeded a threshold value (ca. 0.22 here).

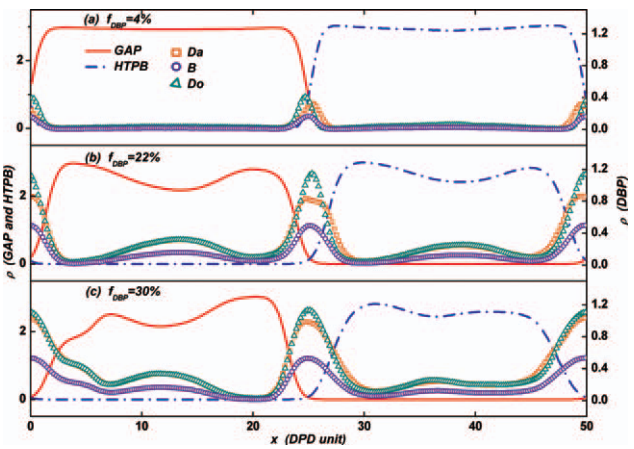

Figure 10 Density profiles for the ternary GAP/HTPB/DBP systems. The *y* axis (right) in the same scale (a–c) is for the homopolymer GAP and HTPB, and the *y* axis (left) is for the plasticizer DBP. [Color figure can be viewed in the online issue, which is available at wileyonlinelibrary.com.]

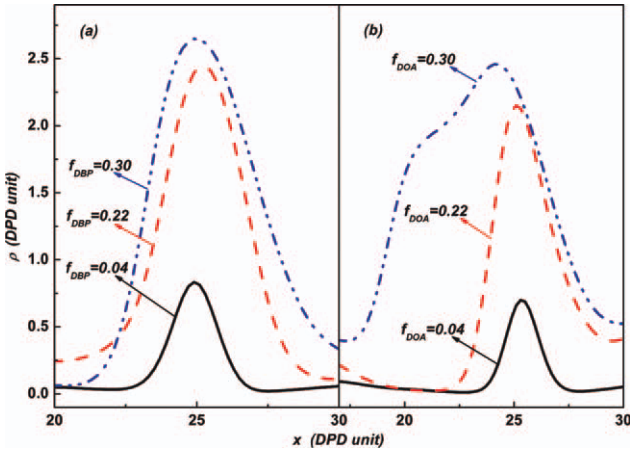

Figure 11 Density profiles for (a) DBP (described by the sum of all beads, $D_a + D_o + B$) and (b) DOA (described by the sum of all beads, $D_a + D_o + D_b$). [Color figure can be viewed in the online issue, which is available at wileyonlinelibrary.com.]

Apparently, the entire results for small molecular plasticizers were in contrast to those of the block copolymer on in reducing γ (see previous discussion). The results can be interpreted as follows: the chain lengths of small molecular plasticizers are far lower than those of the surfactantlike block copolymers. Generally speaking, they easily assembled at the interface and were pressed for the ability to penetrate into the homopolymer phases. The block copolymers were just the opposite and were short on the assembling ability at the interface, although they had a greater penetrability. Therefore, the small molecular plasticizers needed higher penetrabilities to help them decrease γ successively. The longer block copolymers needed higher assembling abilities.

CONCLUSIONS

In this study, DPD simulation methods were used to investigate the interfacial properties of ternary GAP/HTPB/GAP-*b*-HTPB and GAP/HTPB/plasticizers

blend systems. We mainly studied the influence of the long block copolymer and the small molecular plasticizer on the interface of GAP/HTPB by analyzing γ and the density distribution.

For the GAP/HTPB/GAP-*b*-HTPB ternary systems, the addition of a surfactantlike block copolymer reduced γ. However, there was no linear relationship. The analysis results show that the efficiency of the block copolymer with a shorter chain length on reducing γ was higher than that of the block copolymer with a longer chain length only when the concentration $f_{\text{GAP-}b\text{-HTPB}}$ was less than 0.19; the reverse happened when $f_{\text{GAP-}b\text{-HTPB}}$ was greater than 0.19. The main reason was that the efficiency of decreasing γ was determined by the SDs of the block copolymers at the interface. The higher the SDs (i.e., the higher abilities for assembling at the interface) were, the higher the efficiency for reducing γ was. GAP-*b*-HTPB block copolymers with longer chains preferred to orient along the interface. Also, this caused the interfacial densities of longer GAP-*b*-HTPB blocks to increase with the increase of their concentration. Therefore, the SDs of longer GAP-*b*-HTPB blocks at the interface could exceed that of the shorter GAP-*b*-HTPB when $f_{\text{GAP-}b\text{-HTPB}}$ was greater than 0.19.

For the GAP/HTPB/plasticizers ternary systems:

1. The number of coarse-grained beads (GAP- or HTPB-like) was prominent in determining the distribution of the plasticizers; this further influenced the plasticizer efficiency in reducing γ. For example, NG plasticizer only had GAP-like beads; this resulted in the distribution of NG only in the GAP phase and no accumulation at the interface. Therefore, NG plasticizer could not reduce γ of the GAP/HTPB blend.
2. Generally, the small molecular plasticizers with different coarse-grained beads (GAP- and HTPB-like) aggregated easily at the interface. However, they had to possess the ability to penetrate the two homopolymer phases, which ensured that they could reduce γ consecutively with increasing their concentration. For example, DOA plasticizer, with a longer chain length than DBP, had this type of penetrating ability and could successively decrease γ. However, DBP did not have this function.

The authors are grateful to the editors and reviewers for their effective work.

References

1. Teipel, U. Energetic Materials; Wiley-VCH: Weinheim, 2005.
2. Nazare, N.; Asthana, S. N.; Singh, H. J Energy Mater 1992, 10, 43.
3. Vandenberg, E. J. U.S. Pat. 3,645,917 (1972).
4. Provatas, A. Energetic Polymers and Plasticizers for Explosive Formulation—A Review of Recent Advances; DSTO-TR-0966; Defence Science & Technology Organization: Melbourne, Australia, 2000.
5. Selim, K.; Ozkar, S.; Yilmaz, L. J Appl Polym Sci 2000, 77, 538.
6. Kasikc, H.; Pekel, F.; Ozkar, S. J Appl Polym Sci 2001, 80, 65.
7. Selim, K.; Ozkar, S. J Appl Polym Sci 2001, 81, 918.
8. Mohan, Y. M.; Raju, M. P.; Raju, K. M. J Appl Polym Sci 2004, 93, 2157.
9. Manu, S. K.; Sekkar, V.; Scariah, K. J.; Varghese, T. L.; Mathew, S. J Appl Polym Sci 2008, 110, 908.
10. Mathew, S.; Manu, S. K.; Varghese, T. L. Propellants Explosives Pyrotechnics 2008, 33, 146.
11. Mohan, Y. M.; Raju, K. M. Monomers Polym 2005, 8, 159.
12. Mohan, Y. M.; Raju, K. M. Int J Polym Mater 2006, 55, 203.
13. Vasudevan, V.; Sundararajan, G. Propellants Explosives Pyrotechnics 1999, 24, 295.
14. Abou-Rachid, H.; Lussier, L. S.; Ringuette, S.; Lafleur-Lambert, X.; Jaidann, M.; Brisson, J. Propellants Explosives Pyrotechnics 2008, 33, 301.
15. Manu, S. K.; Varghese, T. L.; Mathew, S.; Ninan, K. N. J Propulsion Power 2009, 25, 533.
16. Subramanian, K. Eur Polym J 1999, 35, 1403.
17. Kim, S. H.; Jo, W. H. J Chem Phys 1999, 110, 12193.
18. Diaz-Herrera, E.; Alejandre, J.; Ramirez-Santiago, G.; Forstmann, F. J Chem Phys 1999, 110, 8084.
19. Groot, R. D.; Madden, T. J. J Chem Phys 1998, 108, 8713.
20. Groot, R. D.; Madden, T. J.; Tildesley, D. J. J Chem Phys 1999, 110, 9739.
21. Kong, Y.; Manke, C. W.; Madden, W. G.; Schlijper, G. J Chem Phys 1997, 107, 592.
22. Clark, A. T.; Lal, M.; Ruddock, J. N.; Warren, P. B. Langmuir 2000, 16, 6342.
23. Shillcock, J. C.; Lipowsky, R. J Chem Phys 2002, 117, 5048.
24. Rekvig, L.; Kranenburg, M.; Vreede, J.; Hafskjold, B.; Smit, B. Langmuir 2003, 19, 8195.
25. Maiti, A.; McGrother, S. J Chem Phys 2004, 120, 1594.
26. Tsige, M.; Grest, G. S. J Chem Phys 2004, 120, 2989.
27. Wijmans, C. M.; Smit, B.; Groot, R. D. J Chem Phys 2001, 114, 7644.
28. Qian, H. J.; Lu, Z. Y.; Chen, L. J.; Li, Z. S.; Sun, C. C. J Chem Phys 2005, 122, 184907.
29. Hoogerbrugge, P. J.; Koelman, J. M. V. Europhys Lett 1992, 19, 155.
30. Koelman, J. M. V.; Hoogerbrugge, P. J. Europhys Lett 1993, 21, 363.
31. Español, P. Phys Rev E 1995, 52, 1734.
32. Groot, R. D.; Warren, P. B. J Chem Phys 1997, 107, 4423.
33. Fan, C. F.; Olafson, B. D.; Blanco, M.; Hsu, S. L. Macromolecules 1992, 25, 3667.
34. Schweizer, K. S.; Curro, J. G. J Chem Phys 1989, 91, 5059.
35. Stacer, R. G.; Husband, D. M. Propellants Explosives Pyrotechnics 1991, 16, 167.
36. Mohan, Y. M.; Raju, K. M. Int J Polym Anal Character 2004, 9, 289.
37. Groot, R. D.; Rabone, K. L. Biophys J 2001, 81, 725.
38. Wu, D.-S.; Paddison, S. J.; Elliott, J. A. Energy Environ Sci 2008, 1, 284.